

Gas Phase Photochemistry Can Distinguish Different Conformations of Unhydrated Photoaffinity-Labeled Peptide Ions

Robert E. Bossio, Robert R. Hudgins,[†] and Alan G. Marshall^{*,‡}

Ion Cyclotron Resonance Program, National High Magnetic Field Laboratory, Florida State University, 1800 East Paul Dirac Drive, Tallahassee, Florida 32310-3706

Received: October 31, 2002; In Final Form: January 17, 2003

Peptides containing the chromophore, benzophenone (as the amino acid, 4-benzoyl-phenylalanine (Bpa)), have been synthesized to explore the feasibility of gas-phase photochemical cross-linking to investigate the conformations of unsolvated peptides. The main product of UV irradiation of a BP-containing peptide is CO₂ loss from the peptide C terminus. To test whether decarboxylation results from hydrogen abstraction from acidic residues, we synthesized peptides designed to limit the contact between the Bpa and the peptide C terminus. Such contact is necessary for hydrogen abstraction. The peptide, Ac-Bpa-Ala₁₀-Lys, forms an extended α -helix in the gas phase, thus preventing the N-terminal Bpa from approaching the C terminus.¹ In contrast, Ac-Bpa-Gly₁₀-Lys is a flexible peptide that can adopt multiple “random globule” conformations in the gas phase, some of which could allow contact between the termini and thus photoinduced reaction. On simultaneous UV irradiation of a mixture of both electrosprayed gas-phase peptides in a Fourier transform ion cyclotron resonance ion trap, the degree of decarboxylation is 50-fold less for the α -helical alanine-based peptide than for the flexible glycine-based peptide. The results suggest that intimate contact between the photoexcited Bpa and the C terminus is necessary for decarboxylation, implicating hydrogen atom abstraction as the photochemical mechanism. These results establish the feasibility of probing gas-phase peptide/protein ion conformations by photochemistry of photoaffinity-labeled ions.

Introduction

Photochemical cross-linking is widely used in conjunction with other analytical methods to locate active sites in enzymes and enzyme/substrate binding domains.^{2–5} For example, suppose that a substrate modified with a photochemically reactive moiety (e.g., phenyl azide, diazo ketone, or benzophenone) binds to its cognate enzyme during UV irradiation.² After photoinduced cross-linking, the enzyme is digested, and the fragments containing the modified substrate–peptide complexes may be located by various analytical methods (e.g., chromatographic separation, mass spectrometry). Photoaffinity labeling can reveal binding sites for ATP, inositol, taxol, and other drugs.^{2,3} In a modification of such a protocol, residue contacts with other molecules can be identified by labeling a known amino acid, followed by activation under typical physiological conditions. The self-cross-linked protein is then digested and sequenced, revealing the residue proximities.^{4,5}

Here, we synthesize peptides containing the chromophore, benzophenone (as the amino acid, 4-benzoyl-phenylalanine (Bpa)), to investigate the feasibility of gas-phase photochemical cross-linking experiments to probe protein conformation in the absence of solvent. The main product of UV irradiation of Bpa-containing peptides turns out to be CO₂ loss. To test the hypothesis that CO₂ loss is the result of hydrogen abstraction from the acidic C terminus, we synthesized peptides designed to limit the contact between the Bpa and the peptide C terminus necessary for hydrogen abstraction. The peptide, Ac-Bpa-Ala₁₀-

Lys, is designed to form an extended α -helix in the gas phase, thus precluding direct contact between the N-terminal Bpa and the C-terminal –CO₂H.^{1,6,7} By way of contrast, we prepared Ac-Bpa-Gly₁₀-Lys as a flexible peptide that can adopt multiple “random globule” gas-phase conformations, some of which would allow contact between the N and the C termini and thus photochemical reaction.^{1,2,6–8}

These types of experiments have already proved extremely useful in the study of end-to-end contact formation of solution-phase peptides.^{9,10} Because the degree of photochemical reaction depends on the proximity of the chromophore to the reactive site, measuring the process as a function of peptide length and composition provides a gauge of intramolecular diffusion rates, which can in turn be directly related to the “speed limit for protein folding.”

Decarboxylations have previously been reported for solution phase reactions of targets into which benzophenone groups have been incorporated.^{11–13} Decarboxylation is initiated by the ability of an $n-\pi^*$ triplet excited state to abstract a hydrogen from a C–H bond adjacent to a carboxylic acid or by electron transfer from carboxylate anions.¹⁴ In the present gas phase experiments, electron transfer from carboxylates is unlikely, because all carboxylate groups are protonated. Hydrogen atom abstraction from a C–H bond adjacent to the carboxylic acid groups is a more likely pathway. For a gas phase reaction, however, there could be other routes (e.g., direct H atom abstraction from –CO₂H) leading to decarboxylation. These mechanisms may be investigated in the future.

Experimental Section

One milligram of fibronectin related peptide (FRP) (Sigma Chemical, St. Louis, MO) was dissolved in 500 μ L of *N,N*-

* To whom correspondence should be addressed.

[†] Current address: Department of Chemistry, York University, 4700 Keele St., Toronto, ON M3J 1P3, Canada.

[‡] Member of the Department of Chemistry and Biochemistry, Florida State University, Tallahassee, FL.

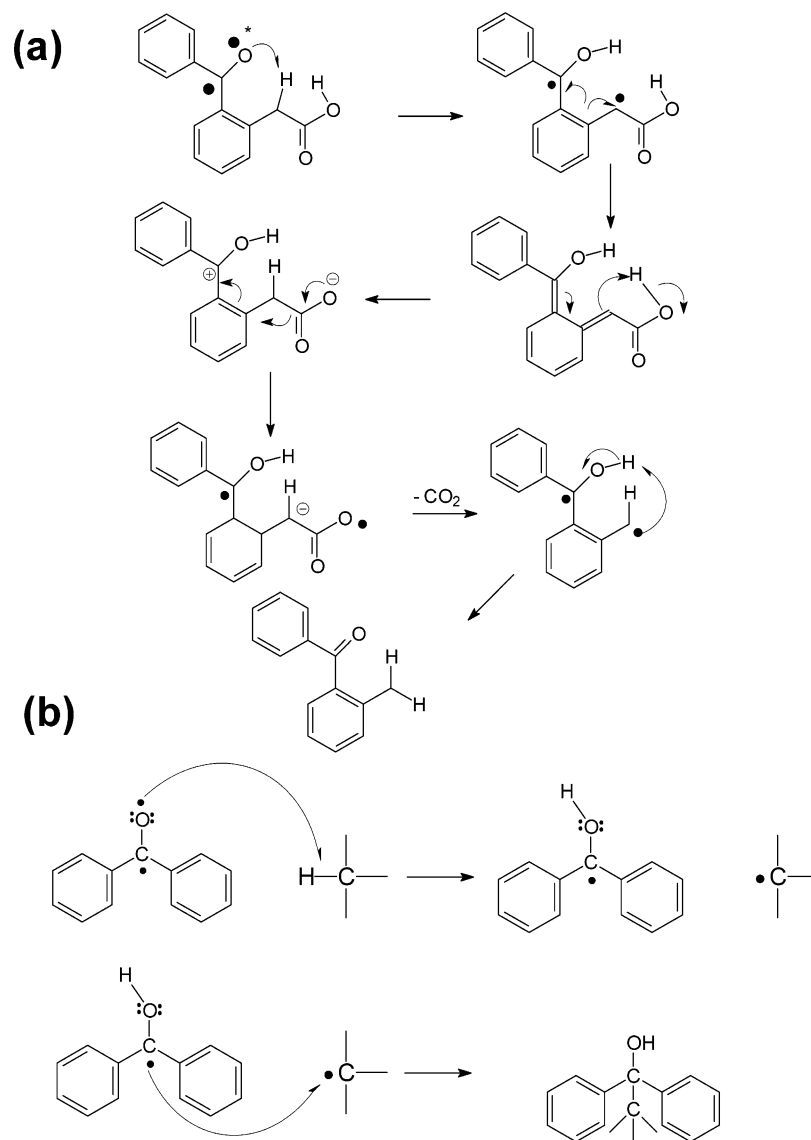


Figure 1. Mechanisms for decarboxylation (a) and cross-linking (b) reactions of benzophenone.^{2,11} In both cases, the reaction is initiated by H atom abstraction by the electrophilic triplet π^* excited state.

dimethylformamide (DMF). Twenty-one milligrams of benzophenone 4-maleimide (BPMal) was dissolved in DMF, and 6 μL of that solution was added to the above FRP solution. The mixture was stirred for 2 days in the dark. Fifty microliters from the reaction mixture was withdrawn and diluted with 50 μL of water and 1 μL of concentrated acetic acid. All solutions were directly infused into the microelectrospray source of a home-built 9.4 T instrument¹⁵ at a flow rate of 500 nL/min.^{16,17} The ESI emitter potential was set to +1.8 kV, with the tube lens voltage set to +0.370 kV. Ions were accumulated in the external octapole region¹⁸ of the 9.4 T instrument for 5 s at an octapole rf frequency of 1.5 MHz and amplitude of 163 Vp-p. All experiments were controlled by a modular ion cyclotron resonance (ICR) data system.^{19,20} $[\text{FRP} + 2\text{H}]^{2+}$ and $[\text{FRP} - \text{BPMal} + 2\text{H}]^{2+}$ conjugate ions were SWIFT-isolated^{21,22} and confined for 400 s without irradiation. Each mass spectrum was derived from four coadded 2-Mword time-domain data sets. The transients were zero-filled once, Hamming apodized, and fast Fourier-transformed (FT),²³ followed by magnitude calculation and two term frequency to m/z converted^{24,25} to yield the final magnitude mode mass-to-charge ratio spectra.

After it was irradiated, the product ion $[\text{FRP} - \text{BPMal} + 2\text{H} - \text{CO}_2]^{2+}$ was SWIFT-isolated and fragmented by sustained

off-resonance irradiation collision-induced dissociation (SORI-CID),²⁶ based on irradiation at 2 kHz below the isotope envelope centroid of the parent ion in the presence of argon (5 μTorr). The calculated maximum center-of-mass ion kinetic energy was 15 eV. Each tandem mass spectrum was derived from four coadded 2-Mword time-domain data sets. The transients were processed as described above.

Ac-Bpa-Gly₁₀-Lys and Ac-Bpa-Ala₁₀-Lys were synthesized by solid phase peptide synthesis in the BASS laboratory of Florida State University. The peptides were dissolved in 1:1:1 water:methanol:formic acid and infused directly into the FT-ICR mass spectrometer by use of a dual electrospray ionization source²⁷ at a flow rate of 500 nL/min. No internal calibrant was used. $[\text{Ac-Bpa-Gly}_{10}\text{-Lys} + \text{H}]^+$ and $[\text{Ac-Bpa-Ala}_{10}\text{-Lys} + \text{H}]^+$ ions were selectively m/z -filtered in a quadrupole mass filter²⁸ prior to octapole accumulation and injection into the ICR cell. The accumulation period for each peptide was adjusted so that the ion magnitudes of the two peptides were approximately equal before UV irradiation.

Photochemical experiments were performed on the trapped peptide ions by use of an Oriel 200 W Hg (Xe) arc lamp equipped with a near-IR water filter, a 324 nm low-wavelength cutoff filter, and a 285 nm low-wavelength cutoff filter. The

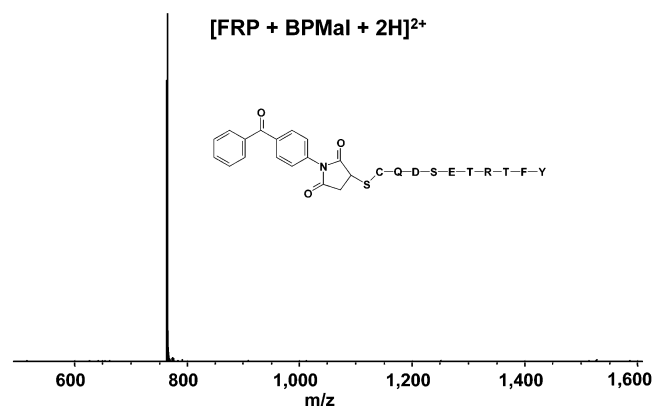


Figure 2. Microelectrospray ionization FT-ICR mass spectrum of FRP photoaffinity-labeled with BPMal. The peptide label conjugate survives electrospray intact.

9.4 T instrument was equipped with an optical grade silica window ~ 1 m from the center of the cell, through which the focused Xe lamp emission was directed. The trapped ions were UV-irradiated for 400, 800, and 1600 s in three separate experiments whose results were coadded four times to yield a final 0.5 Mword time—domain transient. In a blank experiment, ions were held in the trap for 400 s without any UV irradiation.

Molecular dynamics simulations were performed with the Amber3 force field in Hyperchem 5.01. Following a conjugate gradient geometry optimization, molecular dynamics simulations were performed at 300 and 700 K (to explore conformations) for as long as 1 ns. The starting conformation for both peptides was an α -helix. A dielectric constant of 1 was used.

Results and Discussion

Photoinduced Decarboxylation of FRP Ions Photoaffinity-Labeled with BPMal. Our first attempt at gas-phase cross-linking experiments employed FRP, CQDSETRTFY, labeled at its N terminus with BPMal. Benzophenone is known to abstract an H atom from a C—H bond via an electrophilic $n-\pi^*$ triplet excited state, joining the carbon from the benzophenone to the C that has just been H atom abstracted (see Figure 1, bottom).² In a peptide or protein, the final product from the H atom abstraction is a diphenylmethanol group cross-linking two amino acids. Thus, identifying the newly formed C—C bond should be straightforward.

However, recent experiments have demonstrated that the triplet state can also decarboxylate carboxylic acids, starting with H atom abstraction from a CH_2 group adjacent to an RCO_2H (see Figure 1, top). For example, certain drugs containing benzoyl groups can decarboxylate under appropriate conditions.^{11–13,29} In our gas-phase experiments (see below), we observe decarboxylation exclusively.

FRP possesses an N-terminal cysteine, to which BPMal can be attached. The FRP—BPMal conjugate readily electrosprays intact, shown in Figure 2. The results of simultaneous UV irradiation of FRP and its FRP—BPMal conjugate for 400 s (Figure 3) are strikingly different. FRP shows no change in mass, indicating a lack of photochemically induced fragmentation, as expected from the low absorbance above 280 nm for its constituent amino acids. In contrast, the FRP—BPMal peptide shows a mass loss of 43.989 Da to yield abundant product ions, $[\text{FRP} + \text{BPMal} + 2\text{H} - \text{CO}_2]^{2+}$, after ~ 400 s of UV irradiation.

Site of Decarboxylation. FRP has three carboxylic acids, aspartic, glutamic, and the C-terminal carboxylic acid. (Loss of CO_2 is not expected from benzophenone itself.) The SORI-CID spectrum (Figure 4) of the $\text{M}-\text{CO}_2$ product shows that the

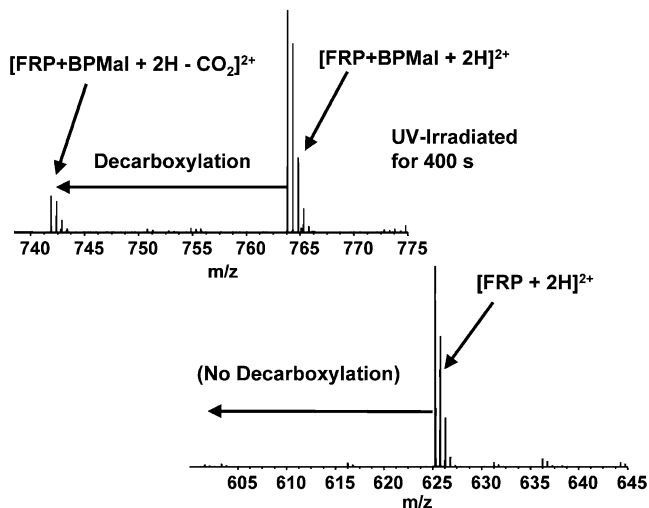


Figure 3. Micro-ESI FT-ICR mass spectrum of FRP and FRP—BPMal UV-irradiated ($\lambda > 324$ nm) simultaneously for 400 s. Although FRP shows no apparent reaction, the FRP—BPMal conjugate shows an obvious loss of CO_2 .

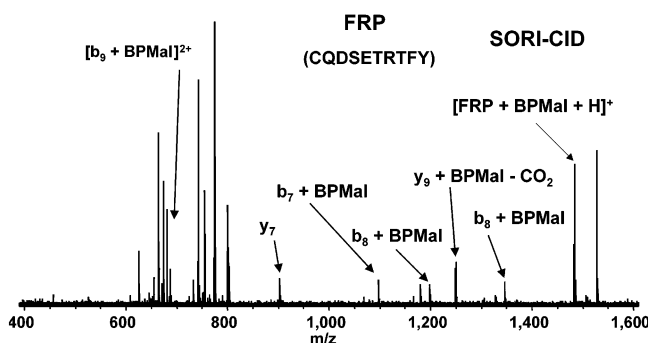


Figure 4. Micro-ESI FT-ICR mass spectrum following SORI-CID of $[\text{FRP} + \text{BPMal} - \text{CO}_2 + 2\text{H}]^{2+}$. These data show that decarboxylation can occur at the carboxyl terminus and at Asp-3 (see text).

carboxy terminus is the primary site of decarboxylation. There is no loss of CO_2 in the b_7 , b_8 , and b_9 ions (each of which contains the D and E residues), and there is loss of CO_2 in the y_9 fragment (which contains the carboxyl terminus). The presence of a y_7 fragment (which contains E and the carboxyl terminus) without decarboxylation shows that decarboxylation can also occur at Asp-3 (which is not present in that fragment). By comparison, the SORI-CID spectrum (not shown) of non-UV-irradiated FRP—BPMal conjugate shows no CO_2 loss, indicating that the decarboxylation is not collisionally induced. Thus, the benzophenone group must be present for photoinduced CO_2 loss.

Next, we must consider various mechanistic alternatives. (i) Does benzophenone need to be near the carboxylic acid to induce CO_2 loss? (ii) Does the FRP—BPMal ion exhibit stable conformation(s) placing the benzophenone close enough to react or is the peptide ion fluxional? (iii) Can the reaction extend to other peptide systems or is it specific to this peptide? To resolve the issue of label proximity, we start from the systems, $[\text{AcAla}_{10}\text{-Lys} + \text{H}]^+$ (a helical and thus relatively rigid peptide in the gas phase) and $[\text{AcGly}_{10}\text{-Lys} + \text{H}]^+$ (a flexible-backbone gas phase peptide), previously investigated by Hudgins and Jarrold,^{7,8} both with and without the benzophenone label.

$[\text{Ac-Bpa-Gly}_{10}\text{-Lys} + \text{H}]^+$ and $[\text{Ac-Bpa-Ala}_{10}\text{-Lys} + \text{H}]^+$. To ensure that adding the benzophenone group does not destroy the α -helical structure of the $\text{Ala}_{10}\text{-Lys}$ motif, we performed molecular dynamic simulations with Hyperchem 5.0. The results are summarized in Figure 5, which shows that the $[\text{Ac-Bpa-}$

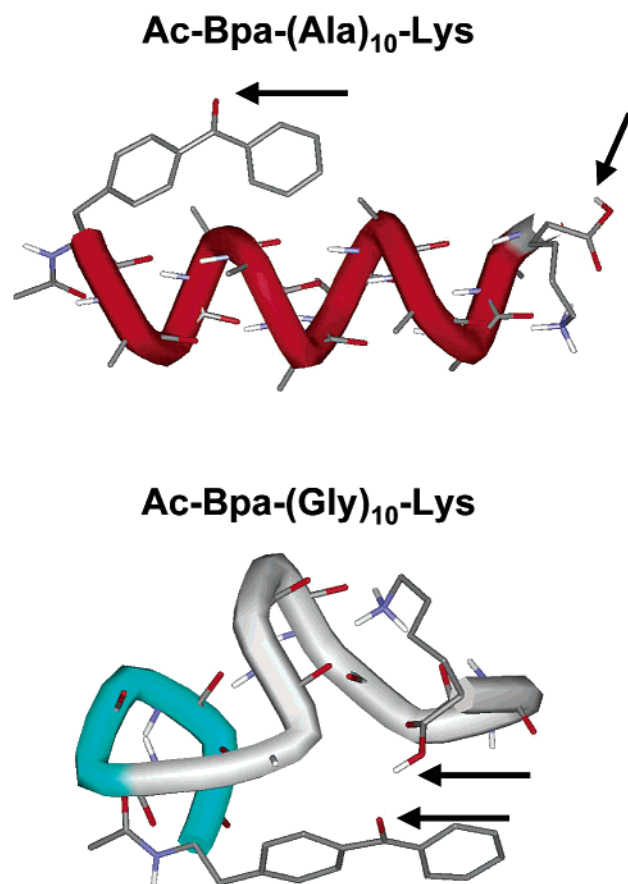


Figure 5. $[\text{Ac-Bpa-Ala}_{10}\text{-Lys} + \text{H}]^+$ and $[\text{Ac-Bpa-Gly}_{10}\text{-Lys} + \text{H}]^+$. These structures were calculated by Hyperchem 5.0. The benzoyl phenylalanine does not disrupt the helical conformation of the $\text{Ala}_{10}\text{-Lys}$ motif, consistent with our experimental results. The $\text{Gly}_{10}\text{-Lys}$ motif, however, possesses at least one conformation, which places the benzoyl phenylalanine close enough to cause the decarboxylation to occur.

$\text{Ala}_{10}\text{-Lys} + \text{H}]^+$ ion maintains its helical conformation even when derivatized as N-terminal benzoyl phenylalanine. In contrast, $[\text{Ac-Bpa-Gly}_{10}\text{-Lys} + \text{H}]^+$ can fold back on itself in any of several ways (one of which is shown).

Figure 6 shows the results of UV irradiating the parent ions $[\text{Ac-Bpa-Gly}_{10}\text{-Lys} + \text{H}]^+$ and $[\text{Ac-Bpa-Ala}_{10}\text{-Lys} + \text{H}]^+$ for 400, 800, and 1600 s, as well as the results of trapping the ions without irradiation. No decarboxylation products are observed for either parent ion in the absence of irradiation, indicating that background gases do not collisionally induce CO_2 loss. Following UV irradiation of both parent ions for 400 s, the prominent product ion, $[\text{Ac-Bpa-Gly}_{10}\text{-Lys} - \text{CO}_2 + \text{H}]^+$, is observed (magnitude is 13% of the total ion signal from the product and parent ion combined magnitudes). For the $[\text{Ac-Bpa-Ala}_{10}\text{-Lys} + \text{H}]^+$ ion and its product $[\text{Ac-Bpa-Gly}_{10}\text{-Lys} - \text{CO}_2 + \text{H}]^+$, the signal magnitude after 400 s of UV irradiation is only 0.6% of the total ion signal magnitude. Figure 7 is an m/z scale expansion of the 400 s irradiation period mass spectrum. After 800 s of UV irradiation, the $[\text{Ac-Bpa-Gly}_{10}\text{-Lys} - \text{CO}_2 + \text{H}]^+$ product increases to 20% vs 1.1% for the $[\text{Ac-Bpa-Ala}_{10}\text{-Lys} - \text{CO}_2 + \text{H}]^+$ product. At 1600 s (Figure 6), the $[\text{Ac-Bpa-Gly}_{10}\text{-Lys} - \text{CO}_2 + \text{H}]^+$ magnitude increases to 30% vs only 2.4% for $[\text{Ac-Bpa-Ala}_{10}\text{-Lys} - \text{CO}_2 + \text{H}]^+$.

The order of magnitude difference between the photoinduced decarboxylation rates of the two photoaffinity-labeled peptides of Figure 6 can be attributed to different conformational flexibility. $[\text{Ac-Bpa-Gly}_{10}\text{-Lys} + \text{H}]^+$ must flex so that its N

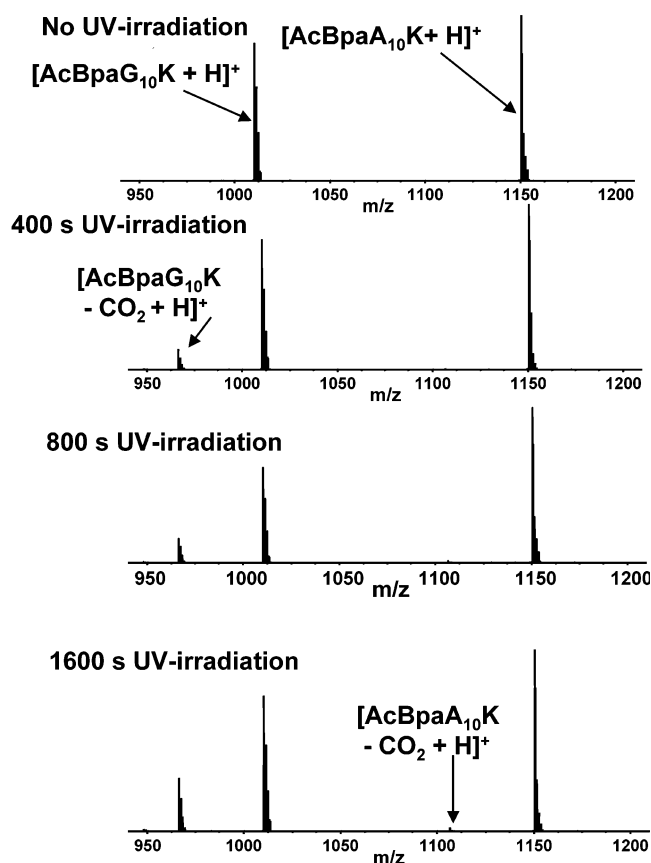


Figure 6. Micro-ESI FT-ICR mass spectra showing $\text{Ac-Bpa-Gly}_{10}\text{-Lys}$ and $\text{Ac-Bpa-Ala}_{10}\text{-Lys}$ irradiated for 0, 400, 800, and 1600 s at $\lambda > 324$ nm. The polyglycine chain shows ready decarboxylation, whereas the polyalanine decarboxylates only slowly. The benzophenone group evidently needs to be near the CO_2H group in the ion for decarboxylation to occur.

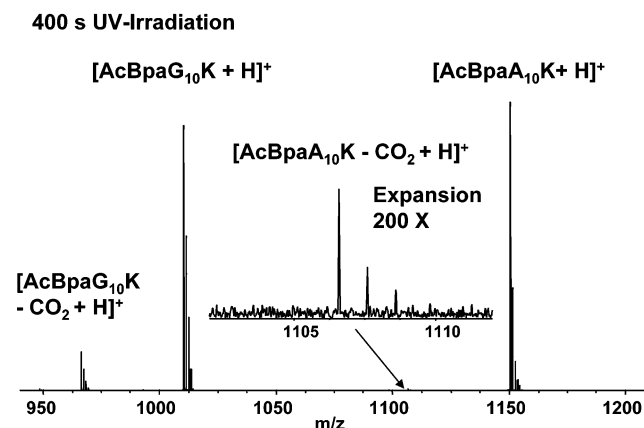


Figure 7. Micro-ESI FT-ICR mass spectrum of $\text{Ac-Bpa-Gly}_{10}\text{-Lys}$ and $\text{Ac-Bpa-Ala}_{10}\text{-Lys}$ irradiated for 400 s, with expanded m/z scale. The spectrum clearly shows the much higher rate of decarboxylation for the conformationally labile $\text{Ac-Bpa-Gly}_{10}\text{-Lys}$ than for the helical (and thus much more rigid) $\text{Ac-Bpa-Ala}_{10}\text{-Lys}$ (see text).

terminus can approach the C terminus (to within a few Angstroms) to allow the electronically excited benzophenone to react with the carboxyl group. That the $[\text{Ac-Bpa-Ala}_{10}\text{-Lys} + \text{H}]^+$ ion decarboxylates at all indicates that either the helical conformation is not indefinitely stable or that the energy from light absorbed by the benzophenone group is internally converted to thermal energy, thereby denaturing the helix.

The relatively slow rate of photoinduced reaction may be attributed in part to the low molar absorptivity ($\epsilon \approx 100$

$M^{-1}cm^{-1}$) for the $n-\pi^*$ transition of benzophenone.² The low molar absorptivity is compensated somewhat by the unit efficiency of intersystem crossing from singlet π^* to triplet π^* . Another factor contributing to slow reaction may be that not all conformations of the Gly₁₀Lys chain bring the benzophenone moiety close to the C terminus for reaction. It has been shown that helix formation in the glycine-based peptides is unfavorable at room temperature because of the many possible globular conformations, resulting in a more favorable conformational entropy for the globular state.⁸ Only a fraction of the possible globular conformations, such as the one shown in Figure 5, will allow contact between the benzophenone moiety and the C terminus.

Ion mobility experiments^{30,31} have previously established the strong helix-forming tendency of gas phase [Ac-Ala₁₀-Lys + H]⁺. The present results offer additional insight. That the [Ac-Bpa-Ala₁₀-Lys + H]⁺ decarboxylates at all may be ascribed to several factors. First, the ion mobility experiments report only an average ion structure. There may be short-lived conformations with enough vibrational energy to unwind and yield a conformation in which the N and C termini come close enough together for the reaction to occur. Second, during the extended UV irradiation period (up to 27 min), ion collisions with background gas may occasionally energize the ion into a new conformation. Third, the energy absorbed by the benzophenone may decay by radiationless modes, also denaturing the helical structure. In any case, the extremely low reactivity of [Ac-Bpa-Ala₁₀-Lys + H]⁺ confirms that its conformation is quite rigid and stable for extended periods of time.

The present experiments were performed with a Xe arc lamp, which produces noncollimated, broadband radiation originating ~1 m away from the ICR cell. Future experiments based on intense, collimated laser light from a XeCl 308 nm excimer laser or a Nd:YAG 3rd harmonic 355 nm laser should provide a higher flux of excitation photons in the ICR cell and greatly reduce the irradiation period.

The mechanism of the present gas-phase reaction is probably similar to that observed in prior solution-phase experiments.^{2,11,12} Although direct H atom abstraction from the O—H bond could be a direct route for CO₂ loss, the O—H bond dissociation energy ($D_{298}^0 \approx 445$ kJ/mol) is much higher than the energy available from the excited $n-\pi^*$ triplet state (~284 kJ/mol).³² Photons of less than 324 nm wavelength are efficiently screened out by the present filter system, eliminating that energy input pathway.

Similar experiments have been performed on peptides in aqueous solution, in which the rate of quenching of photoexcited C-terminal tryptophan by N-terminal lipoate has been measured as a function of peptide sequence and amino acid composition.⁹ A glycine-containing sequence, lipoate-(Ala-Gly-Gln)₃-Trp, is assumed to be a flexible, structureless peptide (similar to Ac-Bpa-(Gly)₁₀-Lys in our experiment), and an alanine-rich sequence, lipoate-(Ala)₂-Arg-(Ala)₄-Arg-Ala-Trp, is assumed to have a high propensity to form α -helical structure (similar to our Ac-Bpa-(Ala)₁₀-Lys). However, it was found that the quenching rate was almost the same for the glycine-containing sequence as for the alanine-rich sequence in solution, in contrast to the 50-fold rate difference in the present gas phase experiments. The peptide length in the Trp-lipoate experiments (11 residues) is similar to that in our experiments (12 residues). However, it is known that even for alanine-based sequences, helix stability is marginal in aqueous solution for short lengths, because the solvent competes for hydrogen bonds with the backbone amides. Our observation of a large rate difference

between short, helix-forming peptides and short, structureless peptides provides further evidence that α -helical peptides are more stable in the gas phase than in aqueous solution.

Conclusions

The present results convincingly establish that a photoinduced gas-phase reaction (in this case, decarboxylation) can in principle distinguish different conformations of gas phase peptides. The technique can obviously be improved by use of brighter, better focused UV irradiation (to reduce the experimental irradiation period) and by development of more conformationally sensitive photoinduced reactions. Such techniques promise to add another tool to the arsenal of methods for probing peptide and protein conformations in the absence of solvent. An obvious extension will be to probe sites of contact in noncovalent complexes (e.g., drug:receptor; protein:protein; etc.), by photoaffinity-labeling a protein at its putative site(s) of interaction with one or more other members of a noncovalent complex. As in condensed phase, photoaffinity labeling has the advantage that it can definitively establish spatial proximity between two sites on the same or bound proteins and the disadvantage that the photoaffinity label may perturb the conformation of the labeled protein. Nevertheless, the wide usage of photoaffinity labeling in solution, combined with the shortage of other methods available in the gas phase, augur well for the future of photochemistry of photoaffinity-labeled peptides and proteins as probes of secondary and tertiary structure and/or mapping of binding sites.

Acknowledgment. We thank Umesh Goli at the BASS laboratory at FSU for synthesizing the peptides used in this study. We also thank Al Stiegman for his generous loan of a Hg(Xe) arc lamp, John Quinn for modifying the 9.4 T ESI FT-ICR mass spectrometer to accommodate these experiments, and Edwin Hilinski for helpful discussions. This work was supported by the NSF National High Field FT-ICR Facility (CHE-99-09502), Florida State University, and the National High Magnetic Field Laboratory in Tallahassee, FL.

References and Notes

- Hudgins, R. R.; Jarrold, M. F. Helix formation in unsolvated alanine-based peptides: Helical monomers and helical dimers. *J. Am. Chem. Soc.* **1999**, *121*, 3494–3501.
- Fleming, S. A. Chemical Reagents in Photoaffinity Labeling. *Tetrahedron* **1995**, *51*, 12479–12520.
- Chatterjee, P. K.; Sternberg, N. L. Using Cell-Fractionation and Photochemical Cross-Linking Methods to Determine the Cellular-Binding Site(S) of the Antitumor Drug Dmp-840. *Photochem. Photobiol.* **1995**, *61*, 360–366.
- Nolansorden, N. L.; Lesiak, K.; Bayard, B.; Torrence, P. F.; Silverman, R. H. Photochemical Cross-linking in Oligonucleotide-Protein Complexes between a Bromine-Substituted 2-5a-Analogue and 2-5a-Dependent Rnase by Ultraviolet Lamp or Laser. *Anal. Biochem.* **1990**, *184*, 298–304.
- Scheefers, H.; Scheefersborchel, U.; Brown, D. T. Photochemical Cross-linking of Lipids in the Membrane of an Enveloped Virus. *Eur. J. Cell Biol.* **1980**, *22*, 160–160.
- Hudgins, R. R.; Mao, Y.; Ratner, M. A.; Jarrold, M. F. Conformations of Gly(n)H(+) and Ala(n)H(+) peptides in the gas phase. *Biophys. J.* **1999**, *76*, 1591–1597.
- Hudgins, R. R.; Ratner, M. A.; Jarrold, M. F. Design of helices that are stable in vacuo. *J. Am. Chem. Soc.* **1998**, *120*, 12974–12975.
- Hudgins, R. R.; Jarrold, M. F. Conformations of unsolvated glycine-based peptides. *J. Phys. Chem. B* **2000**, *104*, 2154–2158.
- Lapidus, L. J.; Eaton, W. A.; Hofrichter, J. Measuring the rate of intramolecular contact formation in polypeptides. *Proc. Natl. Acad. Sci. U.S.A.* **2000**, *97*, 7220–7225.
- Hudgins, R. R.; Huang, F.; Gramlich, G.; Nau, W. M. A Fluorescence-Based Method for Direct Measurement of Submicrosecond Intramolecular Contact Formation in Biopolymers: An Exploratory Study with Polypeptides. *J. Am. Chem. Soc.* **2002**, *124*, 556–564.

- (11) Sobczak, M.; Wagner, P. J. Light-induced decarboxylation of (o-acylphenyl)acetic acids. *Org. Lett.* **2002**, *4*, 379–382.
- (12) Borsarelli, C. D.; Braslavsky, S. E.; Sortino, S.; Marconi, G.; Monti, S. Photodecarboxylation of ketoprofen in aqueous solution. A time-resolved laser-induced optoacoustic study. *Photochem. Photobiol.* **2000**, *72*, 163–171.
- (13) Martinez, L. J.; Scaiano, J. C. Transient intermediates in the laser flash photolysis of ketoprofen in aqueous solutions: Unusual photochemistry for the benzophenone chromophore. *J. Am. Chem. Soc.* **1997**, *119*, 11066–11070.
- (14) Carey, F. A.; Sundberg, R. J. *Advanced Organic Chemistry*; Plenum Press: New York, 1990.
- (15) Senko, M. W.; Hendrickson, C. L.; Pasa-Tolic, L.; Marto, J. A.; White, F. M.; Guan, S.; Marshall, A. G. Electrospray Ionization FT-ICR Mass Spectrometry at 9.4 T. *Rapid Commun. Mass Spectrom.* **1996**, *10*, 1824–1828.
- (16) Emmett, M. R.; Caprioli, R. M. Micro-Electrospray Mass Spectrometry: Ultrahigh-Sensitivity Analysis of Peptides and Proteins. *J. Am. Soc. Mass Spectrom.* **1994**, *5*, 605–613.
- (17) Emmett, M. R.; White, F. M.; Hendrickson, C. L.; Shi, S. D.-H.; Marshall, A. G. Application of Micro-Electrospray Liquid Chromatography Techniques to FT-ICR MS to Enable High Sensitivity Biological Analysis. *J. Am. Soc. Mass Spectrom.* **1998**, *9*, 333–340.
- (18) Senko, M. W.; Hendrickson, C. L.; Emmett, M. R.; Shi, S. D.-H.; Marshall, A. G. External Accumulation of Ions for Enhanced Electrospray Ionization Fourier Transform Ion Cyclotron Resonance Mass Spectrometry. *J. Am. Soc. Mass Spectrom.* **1997**, *8*, 970–976.
- (19) Senko, M. W.; Canterbury, J. D.; Guan, S.; Marshall, A. G. A High-Performance Modular Data System for FT-ICR Mass Spectrometry. *Rapid Commun. Mass Spectrom.* **1996**, *10*, 1839–1844.
- (20) Blakney, G. T.; van der Rest, G.; Johnson, J. R.; Freitas, M. A.; Drader, J. J.; Shi, S. D.-H.; Hendrickson, C. L.; Kelleher, N. L.; Marshall, A. G. Further Improvements to the MIDAS Data Station for FT-ICR Mass Spectrometry. *Proceedings of the 49th American Society on Mass Spectrometry Conference on Mass Spectrometry and Allied Topics*; American Society on Mass Spectrometry: Chicago, IL, 2001; WPM265.
- (21) Marshall, A. G.; Wang, T.-C. L.; Ricca, T. L. Tailored Excitation for Fourier Transform Ion Cyclotron Resonance Mass Spectrometry. *J. Am. Chem. Soc.* **1985**, *107*, 7893–7897.
- (22) Guan, S.; Marshall, A. G. Stored Waveform Inverse Fourier Transform (SWIFT) Ion Excitation in Trapped-ion Mass Spectrometry: Theory and Applications. *Int. J. Mass Spectrom. Ion Processes* **1996**, *157/158*, 5–37.
- (23) Marshall, A. G.; Verdun, F. R. *Fourier Transforms in NMR, Optical, and Mass Spectrometry: A User's Handbook*; Elsevier: Amsterdam, 1990.
- (24) Ledford, E. B., Jr.; Rempel, D. L.; Gross, M. L. Space Charge Effects in Fourier Transform Mass Spectrometry. Mass Calibration. *Anal. Chem.* **1984**, *56*, 2744–2748.
- (25) Shi, S. D.-H.; Drader, J. J.; Freitas, M. A.; Hendrickson, C. L.; Marshall, A. G. Comparison and interconversion of the two most common frequency-to-mass calibration functions for Fourier transform ion cyclotron resonance mass spectrometry. *Int. J. Mass Spectrom.* **2000**, *195/196*, 591–598.
- (26) Gauthier, J. W.; Trautman, T. R.; Jacobson, D. B. Sustained Off-resonance Irradiation for CAD Involving FTMS. CAD Technique that Emulates Infrared Multiphoton Dissociation. *Anal. Chim. Acta* **1991**, *246*, 211–225.
- (27) Flora, J. W.; Hannis, J. C.; Muddiman, D. C. High-mass accuracy of product ions produced by SORI-CID using a dual electrospray ionization source coupled with FTICR mass spectrometry. *Anal. Chem.* **2001**, *73*, 1247–1251.
- (28) Hendrickson, C. L.; Quinn, J. P.; Emmett, M. R.; Marshall, A. G. Quadrupole Mass Filtered External Accumulation for Fourier Transform Ion Cyclotron Resonance Mass Spectrometry. In *Proceedings of the 48th American Society on Mass Spectrometry Annual Conference on Mass Spectrometry and Allied Topics*; MP083, Ed.: Long Beach, CA, 2000; MP083.
- (29) Hasebe, M.; Tsuchiya, T. Photoreductive Decarboxylation of Carboxylic-Acids Via Their Benzophenone Oxime Esters. *Tetrahedron Lett.* **1987**, *28*, 6207–6210.
- (30) Wyttenbach, T.; von Helden, G.; Bowers, M. T. Gas-Phase Conformation of Biological Molecules: Bradykinin. *J. Am. Chem. Soc.* **1996**, *118*, 8355–8364.
- (31) Clemmer, D. E.; Jarrold, M. F. Ion Mobility Measurements and their Applications to Clusters and Biomolecules. *J. Mass Spectrom.* **1997**, *32*, 577–592.
- (32) Lide, D. R., Ed. *CRC Handbook of Chemistry and Physics*; CRC Press: Boca Raton, 1999; Vol. 79.